Materials Physics and Mechanics 13 (2012) 162-174 Received: March 13, 2012

OPTICAL CHARACTERIZATION OF *3D* DISPERSE SYSTEMS WITH NANO- AND MICRO- PARTICLES: POLYMODALITY OF SIZE DISTRIBUTIONS

Alexandra G. Bezrukova*, Olga L. Vlasova

Faculty of Medical Physics and Bioengineering, St. Petersburg State Polytechnical University

Polytekhnicheskaya Street 29, St. Petersburg, 195251, Russia

*e-mail: bezr@PB1097.spb.edu

Abstract. Natural (including biomedical) *3D* disperse systems (DS) with nano- and/or micro-particles are inherently polycomponent polymodal polydisperse systems. Characterization of such systems by different compatible non-destructive optical methods (refractometry, absorbance, fluorescence, light scattering: integral and differential, static and dynamic, unpolarized and polarized) is desirable because of feasibility to organize the on-line testing of their state. At this road it is necessary to take into account peculiarities of inverse optical problem solution for such complex systems (so called "three ill": "ill-defined" *3D* DS, "ill-posed" problems, "ill-conditioned" systems of equations). At the information–statistical approach to the optical characterization and control of *3D* DS it is possible to go round these peculiarities and to qualify the *3D* DS state changes.

1. Introduction

Ensembles of nano- and/or micro- particles can be considered as three-dimensional (*3D*) disperse systems (DS) with particles as a disperse phase and water or air as a dispersive medium [1]. Multiparametric analysis of *3D* DS optical data can provide further progress for detailed characterization and control of *3D* DS with particles of different nature (including biomedical ones). Taking into account optical theory [1-19] and results of experiments [20-34] can help to elaborate sensing elements for on-line control of *3D* DS state. This approach includes:

a) Simultaneous measurements of *3D* DS by different compatible nondestructive (noninvasive) optical methods such as refractometry, absorbance, fluorescence, light scattering (integral and differential, static and dynamic, unpolarized and polarized), and

b) Solution of inverse optical problem by different methods among which are technologies of data interpretation by information-statistical theory [35].

2. Materials and methods

The following water *3D* DS (dispersions, colloids, suspensions) were studied [20-34]: proteins, nucleoproteins, lipoproteids, liposomes, viruses, fat emulsions, milk, perfluorinecarbons-based blood substitutes, antibiotics, nanoparticles of polyaromatic hydrocarbons, cyclodextrins, latexes, liquid crystals, bacterial and another biological cells with various form, size, strains (colibacillus, lactobacillus, thrombocytes, erithrocytes and erythrocyte diagnosticums, lymphocytes and thymocytes, ascite carcinoma cells, etc.), metal

powders, kaolin, kimberlites, zeolites, oils, samples of food and oil products, etc., and mixtures – proteins and nucleic acids, proteins and polymers, liposomes and viruses, liposomes carrying various substances (X-ray contrast agents, metallic particles, enzymes, viruses, antibiotics, etc.), liquid crystals with surfactants, mixtures of colibacillus with kaolin, mixtures of anthracene with cyclodextrin, samples of natural and water-supply waters, air sediments in water, etc. For the solution of inverse optical problem the different approximations of particle form were used such as spheres, prolate and oblate ellipsoids of rotation, core/shell spheres.

The following is short description of main optical methods used for *3D* DS characterization. Abbe and other type *refractometers* were used for determination of medium refractive index, μ_0. Refractive indexes of particles, μ_p , were determined by different special methods which depend on the content and peculiarities of studied *3D* DS. Excitation and emission *fluorescense* spectra [7] were measured at self-made installations and at Hitachi fluorescence spectrophotometer MPF-4A. Extinction of light due to *absorption* and *integral light scattering* was measured with diaphragms at SP-26 (LOMO, St. Petersburg, Russia) and at Schimadzu UV 1205 spectrophotometers. For solution of the inverse optical problem of integral light scattering, the "turbidity spectrum method" or *spectroturbidimetry* (ST) [1,12,14-18] was used. In general, using a spectrophotometer it is possible to measure transmittance of light, T:

$$T = (I_1 / I_0) \cdot 100\% , \tag{1}$$

where I_1 and I_0 is the intensity of transmitted (outgoing through a cuvette) and incident light, respectively. The optical density D (other names: absorbency A, extinction of light E) and turbidity τ are connected with T by the formulas:

$$D = -\lg T = \lg (I_1 / I_0) , \tag{2}$$

$$\tau = -\ln T / l = 2.3\, d / l , \tag{3}$$

where l is the length of optical way (length of a cuvette, in cm).

The light extinction due to the scattering at all angles (except the aperture angle of a photo receiver) is the measure of the integral light scattering. At the interval of wavelength (λ), where there is no absorption of light, $D(\lambda)$ can be considered as the measure of integral light scattering, $D_{sc}(\lambda)$. For the absorbing nanoparticles with a diameter less than λ, at first approximation:

$$D(\lambda) = D_{sc}(\lambda) + D_{abs}(\lambda) , \tag{4}$$

where $D_{sc}(\lambda)$ and $D_{abs}(\lambda)$ is the optical density connected with scattering and absorption, correspondingly.

In a bilogarifmical scale the slope of linear parts of spectra (where there is no absorption of light, usually from 400 nm up to 600 nm) is so called “wavelength exponent”, $n(\lambda)$ [1]:

$$n(\lambda) = -\partial \lg D(\lambda) / \partial \lg \lambda . \tag{5}$$

The function $n(\lambda)$ is the characteristic function [1, 18] of the relative size of particles, α, the relative refractive index of particles, m, and the form of particles:

$$\alpha = \pi\, d\, \mu_0 / \lambda\,, \tag{6}$$

$$m = \mu_p / \mu_0\,, \tag{7}$$

where μ_0 and μ_p are the refractive indexes of dispersive medium and disperse phase (particles), correspondingly;
λ is the wavelength in the middle of a considered interval; for particles in water as dispersive medium $\mu_0 = 1.33$:

$$d = 0.24\, \alpha\, \lambda\,. \tag{8}$$

At the ST d is usually the mean effective equivalent diameter of particles: *effective* diameter means that usually polydisperse polymodal *3D* DS size distributions are approximated as monomodal monodisperse ones [1, 12]; *equivalent* diameter means that form of particles is approximated as a sphere [1]. In the frames of ST there are also approximations as core/shell spheres [14], as ellipsoids of rotation (such forms widely spread in nature among biological particles) with different form parameters – p (equal to axial ratio of large axis to small one). In general, for particle approximation as a rotation ellipsoid, asphericity parameter ε [9] can be used:

$$\varepsilon = a/c, \tag{9}$$

where c is the semiaxis of rotation, a and b are semiaxes perpendicular to c;
for a prolate ellipsoid of rotation $\varepsilon<1$, $a = b < c$ (tables of characteristic functions in [15]),
for an oblate rotation ellipsoid $\varepsilon>1$, $a = b > c$ (tables of characteristic functions in [16]) and
for a sphere $\varepsilon=1$, $a=b=c$ (tables in [18]).
By ST from the tables of characteristic functions $n\ (\alpha, m, \varepsilon)$ [15-18], it is possible to determine α and d or $2c$. In the interval: $2 < n < 4$, n does not depend on m (the result of Mie's theory in this range). If μ_p is known, from $D_{sc}\ (\lambda)$ one can calculate the mean effective equivalent number of particles (N), and the mean effective equivalent disperse phase mass (M).

Numerical calculations according to Mie's theory for model gamma distributions of particles and experiments with bimodal latex suspensions have shown that the mean effective particle radius ($\bar{r}$) determined by ST from $n\ (r)$ calibrations for monodisperse spherical particles corresponds with a minimal error to the relationship [1]:

$$\bar{r} = \sqrt{\overline{r^{n+4}} / \overline{r^{n+2}}}\,. \tag{10}$$

Differential laser static (time averaged) *light scattering* was measured at self-made installation at detector angles from 60 up to 120 degrees, laser wavelength 633 nm, relatively to scattered standards and at ambient conditions. Use of polarizers and retardation element allows obtaining scattering matrix elements [4, 5, 23]. Differential (at detector angle 90 degrees) laser (wavelength 633 nm) static light scattering was also measured at Malvern Autosizer 4700 at temperature 25.0 degree C [31].

In the frames of *dynamic light scattering* **(**DLS**)** method [8] particle size is obtained from the correlation function by using various algorithms for the solution of inverse optical problem. *3D* DS particles are in a random Brownian motion that causes the intensity of scattered light to fluctuate as a function of time. The correlators used in a dynamic light

scattering instruments base on the correlation function of the scattered light intensity of moving particles. That is why this method is called DLS. There are also other titles of this method: *photon correlation spectroscopy*, *quasi-elastic light scattering*, *optical mixing method*, *spectroscopy of intensity fluctuations*.

Auto-correlation function of light scattering intensity, G, predicts the degree of correlation in the signal as a function of the correlation time, t. At approximation of *3D* DS as DS with monomodal monodisperse spherical particle size distribution:

$$G(t) \sim \exp(-2q^2 D_t t), \tag{11}$$

where D_t is the particle translational diffusion coefficient and q is the wave vector defined as:

$$q = (4\pi\mu_0 / \lambda) \sin(\theta/2), \tag{12}$$

where:
λ - wavelength of the incident light (laser wavelength), μ_0 - refractive index of dispersive medium, θ - angle of measurements.

For monomodal monodisperse particle size distribution the particle diameter can be related to the translational diffusion coefficient using Stokes -Einstein equation:

$$d_h = kT / 3\pi\eta D_t, \tag{13}$$

where d_h is the particle hydrodynamic diameter (the Stokes diameter, the Stokes –Einstein diameter, the diameter of sphere that has the same translational diffusion coefficient as the particle); d_h is slightly larger than the geometrical diameter of a sphere due to interaction effects with dispersive medium; k is Boltzmann's constant; T is the absolute temperature; η is the dispersive medium viscosity.

The Malvern Autosizer 4700 with software for evaluation of correlation function [30, 31] and DLS instrument constructed at St. Petersburg Institute of Nuclear Physics with the solution of inverse DLS problem by algorithms based on regularization method were used [19, 20, 27].

3. Results and discussion

Our research [20-34] has investigated different *3D* DS with nano- and/or micro- particles with diameter less than 10 micrometers. The analysis of experimental data for different *3D* DS by compatible optical methods allows draw the conclusion that there are three classes of parameters. The "first class" parameters are measured optical values, for example, intensity values of fluorescence or light scattering under certain conditions (installation conditions, conditions of object treatment, etc.). The "second class" parameters can be calculated from experimental optical data (without any "a priori" information about nature, form and size distribution of particles), for example, "wave exponent" [1] – Formula (5).

The "third class" parameters are parameters of *3D* DS state: mean effective equivalent diameter and number of particles, mean refractive index and mass of disperse phase, number and mass size distributions, parameters of particles structure (form, thickness of shell, core/shell ratio). The "third class" parameters can be obtained after solution of inverse optical problem by using the different algorithms for experimental data processing based on different methods of experimental data interpretation. At this way it is necessary to take into account the *3D* DS inverse optical problem solution peculiarities (so called "three ill").

Firstly, *3D* DS are "ill-defined" systems [1, 17, 18] because difficulties at the solution of direct task connect with the input uncertainty of *3D* DS state parameters (the “third class” parameters). Input data uncertainty is connected with inherent polycomponent content and polydisperse polymodal size distributions of *3D* DS with nano- and/or micro- particles (Fig. 1 through 6, Table 1 and Table 2). Natural *3D* DS (usually as mixtures) are unstable inconstant systems, the state of which can change with changes of external conditions. There are different processes in *3D* DS and their mixtures such as aggregation, disaggregation, debris formation, coalescence, geteroaggregation, sedimentation, flotation and so on. It is important to provide simultaneous measurements by different methods for control of *3D* DS state.

Secondly, inverse tasks for *3D* DS are incorrect or "ill-posed" [2, 3, 13] due to sensitivity of algorithm calculation procedures to small errors of input experimental data. That is why the *regularization* procedures were elaborated [1-3, 10-13] because in practice there is no ambiguous solution of "ill-posed" problems. Incorrect tasks are practically unambiguous, i.e. there are many particle distributions that correspond to similar scattering signal. No one analysis method will meet all needs and even perfect data can not provide a completely accurate particle size distribution. The meaning of average diameter in different methods is different and can be far from geometrical average diameter especially for polymodal size distributions of particles (Fig. 5). The inverse problem incorrectness can often arise from a rather wide problem statement. Making the solution unambiguous by means of additional conditions and restrictions is referred to as regularization of the inverse problem. For example, smoothing the oscillating functions serves as the aim of regularization of the inverse problem of ST [1]. In the ST there is *a priori* refuse from full characterization of the *3D* DS in order to obtain information on averaged properties, such as the mean size of particles, the numerical and mass-volume concentration of a dispersed phase, etc. that, as the experiment suggests, is quite sufficient to solve a number of scientific and technological problems [1].

Thirdly, the systems of linear equations used for inverse problem solution can occur "ill-conditioned" (algebraical term for the cases with very small determinants [2, 3]). For example, the distribution function reconstruction task based on DLS data for *3D* DS comes to a mathematically "ill-conditioned" problem of solving the first type Fredgholm equation with the Lorentz (or exponential) kernel [19].

In Fig. 1 size distributions of kaolin particles obtained by different methods for the same dispersion are presented.

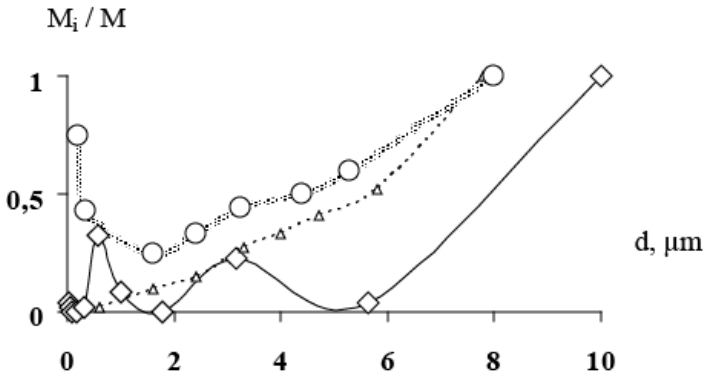

Fig. 1. Kaolin particle mass–size distributions obtained by different methods for the same kaolin dispersion in water:
◊ - dynamic light scattering data based on regularization procedure of distribution retrieval [19]; ○ - combination of spectroturbidimetry with sedimentation; Δ - light microscopy.

Kaolin *3D* DS is usually served as standard of turbidity for water control, but according to the experience [24] size distribution of particles in kaolin dispersions depends on the way of preparation, time of storage, etc. Kaolin *3D* DS is inherently polydisperse and polymodal system.

In Fig. 2 number–size distribution of colibacillus (or Escherichia coli, E.coli) particles obtained by combination of spectroturbidimetry with sedimentation [24] is presented. The "tail" of distribution is the evidence in favor for dividing bacteria or cell aggregates existence in dispersion (similarly particles of influenza virus *3D* DS can be aggregated and size distribution can be bimodal [27]).

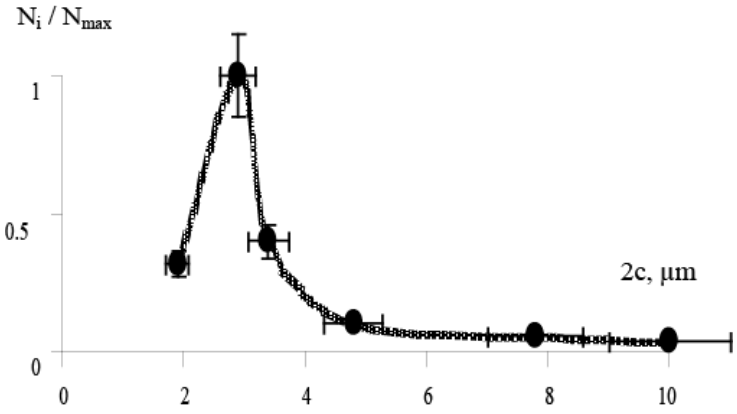

Fig. 2. Number-size distributions of bacteria E. coli (AB 1157) obtained by combination of spectroturbidimetry with sedimentation. Colibacillus cell was approximated as a prolate ellipsoid of rotation with *2c* (large axis of rotation) and asphericity parameter $\varepsilon = a/c = 0.33$ (form parameter $p = c/a = 3$), where *2a* is the axis normal to the rotation axis. The "tail" of distribution is the evidence in favor for dividing bacteria existence in the dispersion.

In Fig. 3 electrophoretical number distributions of kaolin *3D* DS, E.coli *3D* DS and their mixture are presented. The distribution form for mixture is the evidence in favor of kaolin and bacteria geteroaggregation. The size distribution for mixture of kaolin dispersion with colibacillus cells is three modal (if to consider the "shoulder" in mixture number distribution as the third mode belonging to colibacillus cells).

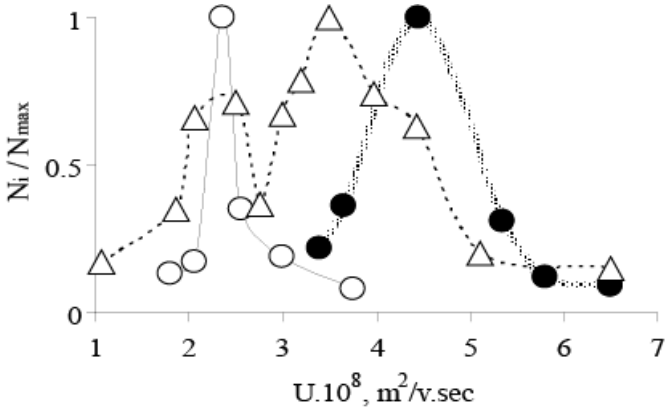

Fig. 3. Electrophoretical number distributions of kaolin *3D* DS (○), E.coli *3D* DS (●) and their mixture (Δ). U is electrophoretical mobility. Form of distribution for mixture is the evidence in favor of kaolin and bacteria geteroaggregation.

In general no one of methods is absolute because the input of modes in the registered signal at various methods can be different depending on parameters of the *3D* DS state. For example, Fig. 4 demonstrates the aggregation process in the dispersion of low density lipoproteids at storage (the first approximation model of atherosclerosis). Both methods, DLS and ST, allow monitoring changes in the state of lipoproteids dispersion. DLS with regularization algorithm allows differentiating not only two main fractions of nano- and micro-particles which diameters differ one from another in about 100 times, but also bimodal size distribution of nanoparticles. At the analysis by ST, bimodal or three modal polydisperse size distributions are approximated by monodisperse monomodal size distributions (Fig. 4, dashed lines). The results allow concluding that the analysis by ST is sensitive to the presence of nanoparticles among microparticles for this *3D* DS.

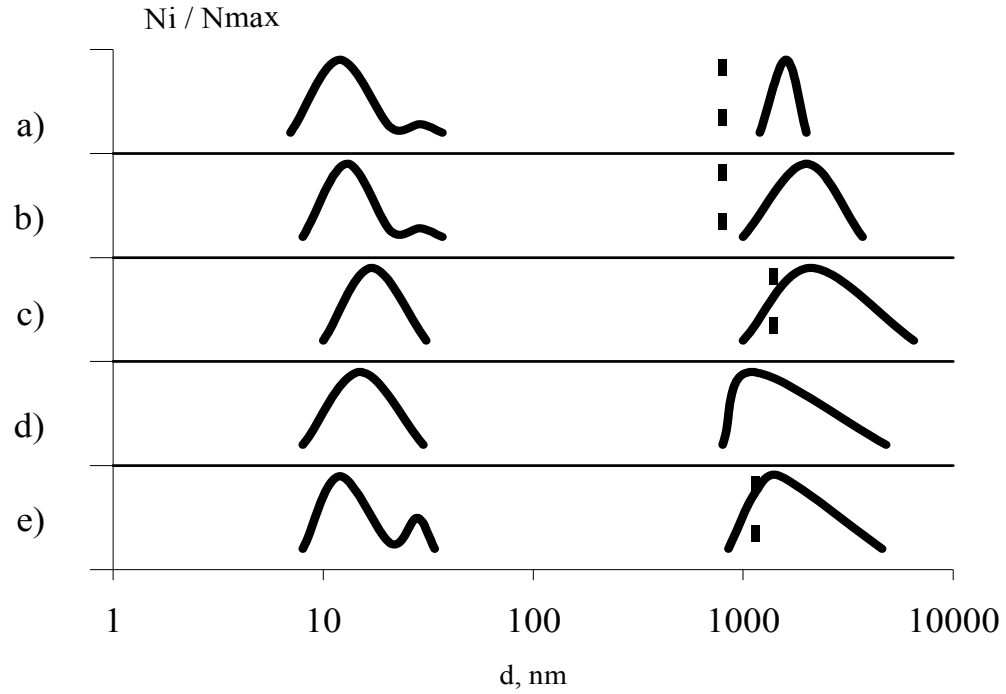

Fig. 4. Number-size distributions for low density lipoproteid particles obtained by dynamic light scattering with regularization algorithm [19] and by spectroturbidimetry (dashed lines) for the same dispersion at storage during: a) 1 day; b) 6 days; c) 26 days; d) 90 days after the formation of sediment in *3D* DS; data for supersediment dispersion (there were not data of spectroturbidimetry for 90 days of storage); e) 120 days, data for supersediment dispersion. Dashed lines (spectroturbidimetry) correspond to monodisperse monomodal size distributions. Diameters (in nm) are presented in the logarithmical scale.

In Table 1 the results of peak analysis by various algorithms in the Malvern photon correlation spectroscopy software for evaluation of correlation function (by intensity, by volume, by number) for latex–water *3D* DS with mean diameter 200 nm (polystyrene nanospheres of Duke Scientific Corporation near the expired date of storage) are presented. In the Table the peak area for one peak resolution is 100 %. Measurement conditions are the following: Malvern Autosizer 4700, registration of DLS at 633 nm, detector angle is 90 degrees, temperature is 25.0 degree C. Here the algorithms are placed in an ascending order of resolution (according to Malvern manual paper): Monomodal (Cumulants) - CONTIN - Multimodal - NNLS (non-negative least squares).

Table 1. Results of peak analysis by various algorithms in the Malvern photon correlation spectroscopy (PCS) software for evaluation of correlation function (by intensity, by volume, by number) for latex–water *3D* DS with mean diameter 200 nm (near the expired date of storage). A1gorithms (A): 1–Monomodal (Cumulants), 2–CONTIN, 3–Multimodal, 4–NNLS (non-negative least squares). Dashed lines correspond to the result of the same latex *3D* DS analysis by spectroturbidimetry: d_{ef} = 150 nm. Diameters (in nm) are presented in the logarithmical scale. Discussion is in the text.

A	By intensity	By volume	By number
1	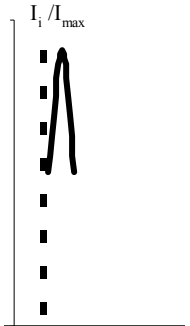	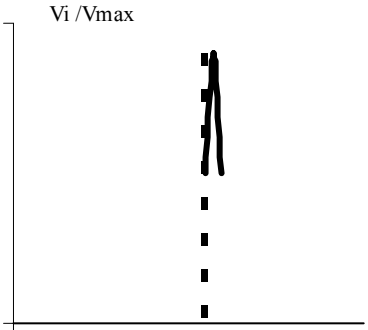	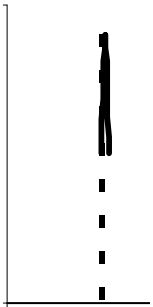
2			
3			
4	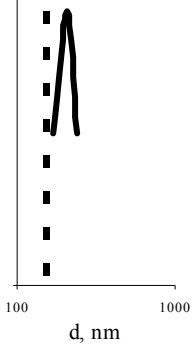	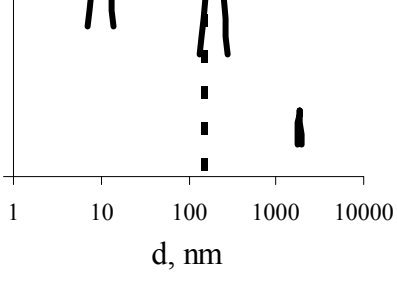	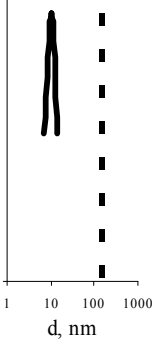

Analysis by intensity (left column) gives the relative intensity of light scattered by particles in each diameter class, and for all algorithms mean diameters and peak widths are approximately the same (only for Multimodal – slightly larger).

For converting intensity distribution to a volume (middle column) and number (right column) distributions using Mie theory, it is necessary to know complex refractive index of particles with real and imaginary parts. If there is no absorption for *3D* DS at 633 nm, the imaginary part of refractive index is about zero. Real part of refractive index for polystyrene nanospheres is 1.59 and relative refractive index is 1.19. Analysis by volume can show the importance of the tail or second peak in real particle size distribution. In Table 1 the Multimodal algorithm allows obtaining bimodal size distribution: latex nanoparticles themselves and their aggregates with larger peak widths and area. NNLS algorithm allows obtaining three-modal size distribution: nano-debris with 10 nm diameters and rather large peak area, latex nano-particles themselves and their aggregates with diameter about two micrometers.

Analysis by number is of limited use because small errors in the data acquisition can lead to huge errors in the distribution by number. In this experiment the results of analysis by number with Monomodal, CONTIN and Multimodal algorithms were in good agreement, but NNLS algorithm allowed obtaining only monomodal size distribution of nano-debris with 10 nm mean diameters (Table 1).

In Table 1 dashed lines correspond to the result of analysis by ST for the same latex *3D* DS. From the ST result, d_{ef} = 150 nm, it is possible to conclude that there are debris in this latex dispersion (the studied polystyrene nanospheres were near the expired date of storage).
In general at peak analysis by intensity, the mean diameter is larger than at analysis by volume, by number and by ST (Table 1). This analysis allows concluding that it is necessary to control the state of latex *3D* DS samples used for calibration of light scattering instruments.

Polydispersity, polymodality and polycomponent content are inherent features of *3D* DS with nano- and micro- particles (Table 2). The probability for each mode existence can be different; some of modes are not “real” modes but “tails” (Fig. 2) or “shoulders” (Fig. 3). For the characterization of size distribution, polydispersity parameter μ can be used ([1], p.130); at that $\mu \to \infty$ and $\mu = 0$ are limiting cases of a monodisperse system and an utmost polydisperse system, correspondingly:

$$\mu = (2.48\, d_m / \Delta d)^2, \tag{14}$$

where Δd and d_m are the width and mode of distribution, respectively; $\Delta d / d_m$ is the relative width of size distribution [1, 18]. *3D* DS with $\mu \approx 200$ are moderately polydisperse and with $\mu < 200$ are essentially polydisperse [18]. Distribution can be approximated with gamma-distribution if it is possible to estimate Δd and d_m [1]. In many cases, the size distribution of polycomponent polymodal polydisperse *3D* DS can be approximated by gamma-distribution [18].

Debris and aggregates of particles can be considered as different components if its refractive indexes are other than the refractive index of initial particles [26]. The form of particles in different modes can be different and such *3D* DS can be considered as polycomponent system. As example, mixture of kaolin dispersion with colibacillus (the first approximation model of natural waters) can be discussed (Fig. 3). According to Fig. 1 and Table 2 kaolin dispersion is MC BM DS or *3D* DS {1;2} and consists of nano- and micro-particles which forms can be differently approximated: nanoparticles can be approximated as spheres, meanwhile microparticles it is better to approximate as oblate ellipsoids of rotation with $\varepsilon = 7$ [24]. Colibacillus (Fig. 2, Table 2) is also MC BM DS or *3D* DS {1;2}.

Table 2. Types of *3D* DS depending on a particle size distribution and component content.

Type of *3D* DS	Abbreviation	Peculiarities	Type of plot (scheme)
Monodisperse	MD	Size distribution is narrow	
Polydisperse	PD	Size distribution is broad	
Monomodal	MM	One peak in a size distribution	
Bimodal	BM	Two peaks in a size distribution	
Polymodal	PM	More than two peaks in a size distribution	
Mono-component	MC	One component in *3D* DS	
Bicomponent	BC	Two components in *3D* DS	
Poly-component	PC	More than two components in *3D* DS	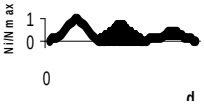
Poly-component Polymodal	PC PM	More than two components in *3D* DS and more than two peaks in a particle size distribution	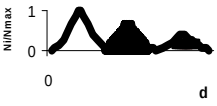
Three component four modal	PC3 PM4 or *3D* DS{3; 4}	Three components in *3D* DS and four peaks in a particle size distribution	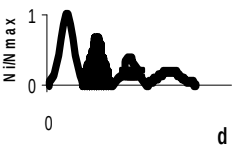

According to Fig. 3 mixture of kaolin dispersion with colibacillus is BC PM DS or *3D* DS{2; 3}, but from the general point of view it is possible to find in such mixture the following fractions: 1) small clay particles, 2) bacteria cells, 3) large clay particles, 4) cells debris, 5) cells aggregates, 6) small clay particles aggregated with cells debris, 7) small clay particles aggregated with bacteria cells, 8) small clay particles aggregated with cells aggregates, 9) large clay particles aggregated with cells debris, 10) large clay particles aggregated with cells, 11) large clay particles aggregated with cell aggregates. If to consider each aggregate fraction as a new component (with new refractive index and form) this mixture can be described as PC9 PM11 DS or *3D* DS {9;11}.

Another *3D* DS can be also analyzed by this way. Mixtures of anthracene and β-cyclodextrin [31,32] nanoparticles in water are bicomponent *3D* DS, which particle size distributions can consist of the several modes: 1) anthracene molecules; 2) β-cyclodextrin molecules; 3) β-cyclodextrin molecules with included anthracene molecules; 4) aggregates (associates) of anthracene molecules; 5) aggregates (associates) of β-cyclodextrin molecules; 6) aggregates (associates) of β-cyclodextrin molecules with anthracene molecules. If to consider each aggregate fraction or fraction with inclusion as a new component (with new refractive index or form) this mixture can be described as PC6 PM6 DS or *3D* DS {6, 6}.

Bovine serum albumin (BSA) *3D* DS are bicomponent [33] (protein molecules and impurities, mainly lipids) polymodal *3D* DS, which particle size distribution can consist of the following modes (Fig. 5): 1) BSA molecules; 2) lipid molecules; 3) aggregates (associates) of BSA molecules; 4) aggregates (associates) of lipid molecules; 5) aggregates (associates) of BSA molecules with lipid molecules.

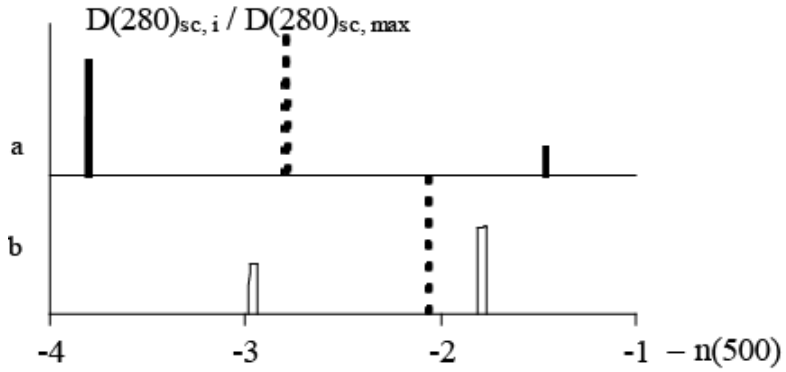

Fig. 5. Dependencies of $D(280)_{sc,i}/D(280)_{sc,max}$ from – n (500), analogously to Fig. 4, for bovine serum albumin dispersions (BSA, [33]) obtained by spectroturbidimetry (ST, dashed lines) and by combination of ST with sedimentation. All data correspond to monodisperse monomodal distributions: a) data for BSA (Reachim), b) data for BSA (Fluka).

The BSA *3D* DS can be characterized as PC5 PM5 DS or 3D DS {5, 5}. In Fig. 5 data for two preparations of BSA *3D* DS [33] are presented. Dependence of "$D\ (280)_{sc,\ i}$ / $D\ (280)_{sc,\ max}$" from "– n (500)" is some sort of analog of Fig. 4, because "– n (500)" is connected with diameter of particles and the value "$D\ (280)_{sc,\ i}$ / $D\ (280)_{sc,\ max}$" is connected with relative number of particles. $D\ (280)_{sc,\ max}$ is the value for initial dispersion obtained by ST. $D\ (280)_{sc,\ i}$ can be obtained by combination of ST with sedimentation for analysis of initial dispersion. By such way one can find approximately the main modes existence in the *3D* DS in the frames of ST. All data correspond to monodisperse monomodal distributions. It can be seen that for BSA (Fluka) the difference between positions of 2 modes is larger than for BSA (Reachim).

Optical parameters can reflect most changes in the state of such complex systems. One of the important problems is the interpretation of mixtures optical signal on the presence the

component of interest without any *a priori* information about *3D* DS. In Fig. 6 the results of DLS inverse problem solution by regularization algorithm [19] for sample of water-pump water sediments are presented. To which components these three modes are belonged?

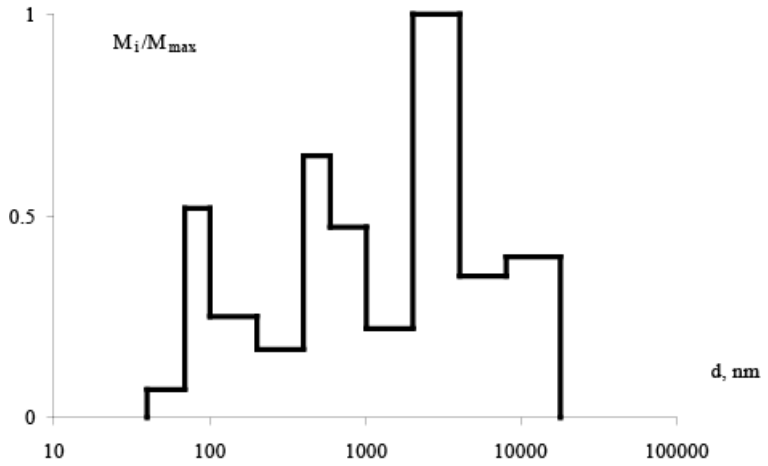

Fig. 6. Dynamic Light Scattering (DLS) data (with regularization algorithm for inverse optical problem solution [19]) for a sample of water-pump water sediments. Diameters (in nm) are presented in the logarithmical scale.

4. Conclusions and future outlook

The experience suggests that the set of optical parameters of so called "second class" can be unique for each *3D* DS [21, 22, 29]. Optical parameter sets (*N*-dimensional vectors [29]) can reflect in "unobvious" form all peculiarities of *3D* DS: nature (constituent substances), form, inner and surface structure of particles, distributions of particle size, number, mass, refractive index, form, structure, etc., tendencies (liability) to aggregation, disaggregation, inclusion [31, 32], coalescence, geteroaggregation, sedimentation, flotation, changes in the state of mixtures, etc. Due to the fusion of various optical data and by information statistical theory [35] it is possible to find the set of the most informative parameters, to increase sensitivity of *3D* DS state differentiation by optical *on-line* measurements, to solve the inverse optical problem on the presence of a component of interest in mixtures and on the nature of particles. The information–statistical approach to the inverse problem solution suggests a refuse from any regularization (refuse from any *a priori* information about *3D* DS). This approach can be considered as an integral one for the study of the system at the moment of measurements as a single whole intact nondestructive unity with the minimum interference. Combination of information–statistical method with other methods can help to investigate the processes in *3D* DS. It can demonstrate an awareness of potential applications for bio- and nano-technology, drug delivery, colloid science, etc. and for protection of environment.

Authors would like to thank Prof. Dr. L.M. Molodkina, Dr. T.G. Braginskaya and Prof. Dr. V.V. Klubin for the help with experiments and useful discussions.

References

[1] V.J. Klenin, *Thermodynamics of Systems Containing Flexible Chain Polymers* (Elsevier, 1999).

[2] K.S. Shifrin, G. Tonna, In: *Advances in Geophysics*, ed. by R. Dmowska, B. Saltzman, (Academic Press, 1993), Vol. 34, p.175.

[3] K.S. Shifrin, *Atmospheric Aerosols, Methods of Analysis* (Oregon State University, 1996).

[4] C.F.Bohren, D.R.Huffman, *Absorption and Scattering of Light by Small Particles* (Wiley, New York, 1983).
[5] Light Scattering by Nonspherical Particles. Theory, Measurements and Applications, ed. by M.I. Mishchenko, J.W. Hovenier, L.D. Travis, AP, 1999, 690 pp.
[6] E. Zubko, Yu. Shkuratov, K. Muinonen, G. Videen // *Journal of Quantitative Spectroscopy and Radiative Transfer* **100** (2006) 489.
[7] J.R. Lakowicz, *Principles of fluorescence spectroscopy* (Plenum Press, New York and London, 1983).
[8] H.Z. Cummins, E.R. Pike, *Photon Correlation and Light Beating Spectroscopy* (Plenum Press, London, 1977).
[9] V.N. Lopatin, F.Ya. Sid'ko, *Introduction in Optics of Cell Suspensions* (Siberian Branch of Nauka Publishing House, Novosibirisk, 1988), in Russian.
[10] H. Schnablegger, O. Glatter // *Appl. Opt.* **30** (1991) 4889.
[11] O.V. Dubovik, T.V. Lapyonok, and S.L. Oshchepkov // *Appl. Opt.* **34** (1995) 8422.
[12] S.Yu. Shchyogolev // *J. Biomed. Opt.* **4 (**1999) 490.
[13] I. Veselovskii, A. Kolgotin, V. Griaznov, D. Müller, U. Wandinger, D. N. Whiteman // *Appl. Opt.* **41** (2002) 3685
[14] Yu.I. Kutuzov, V.J. Klenin // *Optika i Spectroskopiya* **55** (1983) 383.
[15] N.G. Khlebzov, S.Yu. Shchyogolev // *Optika i Spectroskopiya* **42** (1977) 1152.
[16] N.G. Khlebzov, S.Yu. Shchyogolev, V.J. Klenin // *Optika i Spectroskopiya* **45** (1978) 563.
[17] N.G. Khlebzov, S.Yu. Shchyogolev, V.J. Klenin, S.Ya. Frenkel // *Optika i Spectroskopiya* **45** (1978) 710.
[18] V.J. Klenin, S.Yu. Shchyogolev, V.I. Lavrushin, *Light Scattering Characteristic Functions of Disperse Systems* (Saratov University Publishing House, Saratov, 1977), in Russian.
[19] T.G. Braginskaya, P.D. Dobichin, M.A. Ivanova, V.V. Klyubin, A.V. Lomakin, V.A. Noskin, G.E. Shmelev, S.P. Tolpina // *Physica Scripta* **28 (**1983)73.
[20] V.V. Klubin., T.G. Braginskaya, A.S. Kuznetsov, A.G. Bezrukova, V.M. Kolikov // *Kolloidnii zhurnal*, **51 (**1989) 376.
[21] A.G. Bezrukova //*Progr. Colloid Polym. Sci*. **93** (1993) 186.
[22] A.G. Bezrukova // *Proc. SPIE* **3107** (1997) 298.
[23] A.G. Bezrukova //*Mater. Res. Soc. Proc.* **711** (2002) FF7.9.
[24] O.L. Vlasova and A.G. Bezrukova // *Proc. SPIE* **5127** (2003) 154.
[25] A.G. Bezrukova // *European Cells and Materials Journal* **6,** *Supplement 1* (2003) 88.
[26] A.G. Bezrukova // *Proc. SPIE* **5400** (2004) 189.
[27] A.G. Bezrukova // *Proc. SPIE* **5831** (2005) 112.
[28].A.G. Bezrukova // CD: *2006 Spring National Meeting Conference Proceedings*, New York: AIChE, 2006.
[29] A.G. Bezrukova // *Proc. SPIE* **6253** (2006) 62530C-1
[30] A. Bezrukova, M. Lubomska, P. Magri, M. Rogalski // *Proc. SPIE* **6597** (2007) 65970M.
[31] A. Bezrukova, M. Lubomska, M. Rogalski // *Rev. Adv. Mater. Sci*. **20** (2009) 70.
[32] A. G. Bezrukova, *Proc. SPIE* **7377** (2009) 73770B-1.
[33] A.G. Bezrukova, O.L. Vlasova // *Materials Physics & Mechanics* **9** (2010) 167.
[34] A.G. Bezrukova // *European Cells and Materials Journal* **20,** *Supplement 3* (2010) 19.
[35] F.M. Goltsman, *Physical Experiment and Statistical Conclusions* (Leningrad University Publishing House, Leningrad, 1982), in Russian.